arXiv:1610.01114v1 [q-bio.QM] 4 Oct 2016

Efficient estimation of the maximum metabolic productivity of batch systems

Peter C. St. John[1], *Michael F. Crowley*[1], *Yannick J. Bomble*[1]

[1]Biosciences Center, National Renewable Energy Laboratory, Golden CO 80401

Abstract

Background

Production of chemicals from engineered organisms in a batch culture involves an inherent trade-off between productivity, yield, and titer. Existing strategies for strain design typically focus on designing mutations that achieve the highest yield possible while maintaining growth viability. While these methods are computationally tractable, an optimum productivity could be achieved by a dynamic strategy in which the intracellular division of resources is permitted to change with time. New methods for the design and implementation of dynamic microbial processes, both computational and experimental, have therefore been explored to maximize productivity. However, solving for the optimal metabolic behavior under the assumption that all fluxes in the cell are free to vary is a challenging numerical task. Previous studies have therefore typically focused on simpler strategies that are more feasible to implement in practice, such as the time-dependent control of a single flux or control variable.

Results

This work presents an efficient method for the calculation of a maximum theoretical productivity of a batch culture system using a dynamic optimization framework. The proposed method follows traditional assumptions of dynamic flux balance analysis: first, that internal metabolite fluxes are governed by a pseudo-steady state, and secondly that external metabolite fluxes are dynamically bounded. The optimization is achieved via collocation on finite elements, and accounts explicitly for an arbitrary number of flux changes. The method can be further extended to calculate the complete Pareto surface of productivity as a function of yield. We apply this method to succinate production in two engineered microbial hosts, *Escherichia coli* and *Actinobacillus succinogenes*, and demonstrate that maximum productivities can be more than doubled under dynamic control regimes.

Conclusions

The maximum theoretical yield is a measure that is well established in the metabolic engineering literature and whose use helps guide strain and pathway selection. We present a robust, efficient method to calculate the maximum theoretical productivity: a metric that will similarly help guide and evaluate the development of dynamic microbial bioconversions. Our results demonstrate that nearly optimal yields and productivities

can be achieved with only two discrete flux stages, indicating that near-theoretical productivities might be achievable in practice.

Keywords

flux balance analysis, dynamic optimization, elementary flux modes, *Actinobacillus succinogenes*, *Escherichia coli*

Background

Microbial bioconversion plays a critical role in efforts to enable sustainable production of commodity chemicals from renewable feedstocks. The economic feasibility of the integrated biorefinery concept therefore hinges sharply on the productivity, yield, and titers that can be achieved by a given microbial host [Davis et al., 2013]. Flux balance modeling has emerged as an important tool in guiding experimental efforts in strain design by predicting the effects of gene knockouts and overexpression on metabolite yields [Feist et al., 2009]. In developing engineered organisms for optimal performance in batch cultures, A trade-off is often encountered between the productivity and yield that can be obtained via metabolic interventions [Holtz and Keasling, 2010]. As a result, many existing strategies for strain design involve designing mutations to achieve the highest yield possible while maintaining growth viability [Burgard et al., 2003, Ranganathan et al., 2010]. Other strategies have specifically addressed the importance of productivity through dynamic simulations [Zhuang et al., 2013, Hanly and Henson, 2013]. Overall, approaches tend to follow the principle of designing static networks with minimum metabolic functionality to achieve desired yields [Ruckerbauer et al., 2014]. While these methods are computationally and experimentally tractable, optimum productivity is likely achieved by a dynamic strategy, in which the partition of resources between biomass and product formation varies with time [Venayak et al., 2015].

Experimental studies have investigated the use of multi-stage fermentations to increase productivity and/or yield. These techniques range from simple manipulations, such as changing from aerobic to anaerobic conditions [Andersson et al., 2007], to more complex genetic toggle switches [Soma et al., 2014] or otherwise inducible gene expression [Valdez-Cruz et al., 2010]. Computational methods have also been developed to aid in optimizing two-stage fermentation systems. Gadkar *et al.* optimized the flux profile of glycerol kinase to maximize the productivity of glycerol from glucose [Gadkar et al., 2004]. Similarly, Anesiadis and coworkers proposed an extension to Gadkar's work, where parameters for a quorum-sensing toggle switch are tuned to provide the optimal repression for a target gene to maximize ethanol productivity [Anesiadis et al., 2008]. However, since these systems prioritize experimental tractability (by choosing a single reaction target as their control strategy), they do not guarantee that the optimized productivity reaches the global maximum.

The calculation of maximum theoretical yield is well established in the metabolic engineering literature, and its use helps guide strain design and pathway selection for static knockout and/or overexpression efforts. Maximum yields are useful even though they are not physically realizable: they reveal the cofactor balancing and pathway split ratios necessary to achieve optimum carbon conservation. In an analogous fashion, an estimate of the maximum theoretical productivity of a batch culture system would prove equally useful for the growing field of designing dynamic metabolic interventions. However, due to the computational burden associated with such an estimate, no generalized framework for optimizing over all feasible flux profiles currently exists.

In this article, we present an efficient method for calculating the maximum theoretical productivity of a batch system based on dynamic optimization [Biegler, 2007]. In this approach, a dynamic system representing the changes in metabolite concentration over time is represented by a collection of interpolating polynomials that divide the time domain into a set of finite elements. The polynomials are constrained to be continuous between each finite element, and at each of a set of defined points, constraints are imposed to ensure

the derivatives of the interpolating polynomials are consistent with maximum substrate uptake rates and maintenance requirements. In this manner, optimal metabolite profiles are found in a single optimization using a large-scale nonlinear programming solver. Dynamic optimization has previously been used in metabolic modeling, including in an early study on dynamic flux balance analysis (DFBA) [Mahadevan et al., 2002] and in calculating optimal control for fed-batch fermentations [Hjersted and Henson, 2006]. However, its widespread usage has been limited by the number of variables that can be simultaneously considered. In this study, we remove the explicit mass balance constraints by calculating elementary flux modes [Schuster et al., 1999], and reduce the dimensionality of the optimization problem using yield analysis [Song and Ramkrishna, 2009]. Our method accounts explicitly for an arbitrary number of fermentation stages, and allows metabolic fluxes to change continuously over the course of the entire simulation. Since productivity and yield cannot be simultaneously maximized, we demonstrate how this method can be easily extended to calculate the complete productivity vs. yield Pareto frontier. We apply our method to succinic acid production in two microbial hosts: engineered *Escherichia coli* and native *Actinobacillus succinogenes*. Succinic acid is a precursor to commodity chemicals in several industries, and a promising intermediate in the development of sustainable chemical production routes [Song and Lee, 2006]. We show that the method can be useful in strain choice by comparing optimal productivity-yield surfaces for two organisms, and further demonstrate that nearly optimal yields and productivities can be achieved with only two discrete flux stages.

Methods

Dynamic flux balance analysis

In flux balance analysis (FBA) models, intracellular metabolic reactions are represented by a stoichiometric matrix $\mathbf{S}$, such that S_{ij} represents the quantity of metabolite j produced (or consumed) by reaction i. Fluxes through each reaction are represented by the vector $\mathbf{v}$. It is assumed that the time scales associated with intracellular metabolite equilibria are much faster than those associated with cell growth or changes to external metabolite concentrations, and therefore that metabolites in the cell can be modeled using a pseudo-steady-state approximation, $\mathbf{Sv} \approx \mathbf{0}$.

FBA models can be extended to consider the dynamics of substrate consumption and biomass formation by including specific bounds on exchange fluxes and allowing the accumulation of depletion of external metabolites. The dynamic system for cell growth considered in this paper is

$$\frac{dx_i(t)}{dt} = v_i(t)\ x_0(t) \quad \text{for } i \in [0, N_X], \tag{1}$$

where $\mathbf{x}(t)$ represents the concentration of external boundary species, chosen such that $x_0(t)$ is the concentration of dry cell weight (DCW, in grams), and $\mathbf{v}(t)$ represents the flux through each reaction in the cell (in mmol g_{DCW}^{-1} hr^{-1}), chosen such that $v_0(t)$ through v_N represent the exchange flux for species x_0 through x_N, respectively. The flux through the first reaction is therefore the specific growth rate ($v_0(t) \equiv \mu(t)$), and is in units of hr^{-1}. The resulting dynamic flux balance analysis (DFBA) model takes the form of an ordinary differential equation with an embedded linear program, for which efficient methods for the solution of the initial value problem have been developed [Höffner et al., 2012].

The objective considered in this paper is to maximize productivity of the desired metabolite, x_p, by finding the optimum intracellular fluxes profiles $\mathbf{v}(t)$ and final fermentation time t_f; subject to steady-state constraints, reaction reversibility, and substrate uptake:

$$\begin{aligned} &\max_{\mathbf{v}(t), t_f} \frac{x_p(t_f) - x_p(t_0)}{t_f} \\ \text{such that} \quad &\mathbf{Sv}(t) = 0, \\ &\mathbf{v_{lb}}(t) \le \mathbf{v}(t) \le \mathbf{v_{ub}}(t) \end{aligned} \tag{2}$$

The optimization in eqns. 1, 2 therefore takes the form of an optimal control problem, which can be solved by discretizing in time and solving the problem using dynamic optimization. In previous applications of dynamic optimization in DFBA models, intercellular fluxes are either optimized directly [Hjersted and Henson, 2006] or replaced with representative input-output reactions found via pathway analysis [Mahadevan et al., 2002]. In this study, we take advantage of the productivity objective to select Pareto-optimal pathways, greatly reducing the dimensionality of the optimization.

Calculation of elementary flux modes

To select the optimal metabolic pathways, we calculate elementary flux modes (EFMs) for both of the considered metabolic networks. An EFM is a vector $\mathbf{r}$ in the right nullspace of $\mathbf{S}$ ($\mathbf{Sr} \equiv 0$), such that no other elementary mode has nonzero entries that are a subset of the nonzero entries of r_i [Schuster et al., 1999, Jevremovic et al., 2010]. EFMs contain the important property that any vector in the right nullspace of $\mathbf{S}$, i.e. any feasible steady-state flux, can be expressed as a nonnegative combination of the elementary modes $\mathbf{r}$ [Terzer and Stelling, 2008]. Because of this property and because we are only interested in the effect of an elementary mode on the maximum productivity, we can condense the complete set of EFMs to a convex hull in the projection in which we are interested [Song and Ramkrishna, 2009]. We further restrict our analysis to the Pareto front of EFMs which allow optimum productivity, removing inefficient modes without affecting the optimal solution.

Dynamic optimization

We find the flux profiles that achieve the maximum productivity via orthogonal collocation on finite elements, a method for solving end-point problems involving a dynamic system without an embedded ODE integrator [Biegler, 2007]. In the method, the dynamic system is represented by a series of algebraic constraints that implement an implicit Runge-Kutta method. The resulting sparse nonlinear program is then solved via a large-scale nonlinear programming (NLP) solver. Following the approach of orthogonal collocation [Biegler, 2010], we represent the state variables $\mathbf{x}(t)$ from eq. 1 as a collection of Lagrange interpolating polynomials. A summary of the dimensions and variables used in this method are presented in Tables 1, 2.

Table 1: Dimensions of the NLP problem.

Dimension	Index	Description
N_X	i	Number of state variables
N_K	j	Number of finite elements
N_D	k	Degree of collocation polynomials
N_F	l	Number of fermentation stages
N_R	m	Number of elementary flux modes

Table 2: Variable matrices optimized by nonlinear programming. These matrices are flattened to a single parameter vector prior to being passed to IPOPT.

Variable	Shape	Description
$\mathbf{X}$	(N_X, N_K, N_D)	Nodes of the Legendre polynomials interpolating $\mathbf{x}(t)$
$\mathbf{Y}$	(N_F, N_R)	Fractional expression of each elementary mode by stage
$\mathbf{A}$	(N_K, N_D)	Total flux at each collocation point
$\mathbf{h}$	(N_F)	Length of each of the finite elements within a stage

The time domain t of the fermentation is divided into N_K finite elements with a non-dimensionalized internal time $\tau \in [0, 1]$. Within each finite element, we represent the state vector by a polynomial of degree

N_D at $N_D + 1$ collocation points, denoted τ_n. We use Gauss-Radau collocation for its stiff decay, and therefore for $N_D = 5$, we set $\tau_k \in \{0, 0.06, 0.28, 0.58, 0.86, 1.00\}$:

$$\begin{aligned} \mathbf{x}_j(\tau) &= \sum_{k=0}^{N_D} \boldsymbol{\ell}_k(\tau)\mathbf{x}_{jk} \\ \text{where} \quad \boldsymbol{\ell}_k(\tau) &= \prod_{n=0,\, n\neq k}^{N_D} \frac{\tau - \tau_n}{\tau_k - \tau_n} \end{aligned} \tag{3}$$

To model changes in the flux distribution, the finite elements are allocated between N_F distinct fermentation stages. Within each stage we assume the fractional distribution of elementary modes is held constant while the total flux through the system is allowed to vary. The dynamic system can thus be calculated by:

$$\frac{d\mathbf{x}_{ij}}{dt} = \frac{1}{h_l}\frac{d\mathbf{x}_{ij}}{d\tau} = a_{jk}x_{0jk}\mathbf{R}\ \mathbf{y}_l \tag{4}$$

in which $\mathbf{R}$ is a matrix of shape (N_R, N_X) that contains the chosen elementary modes; $\mathbf{y}_l$ contains the fractional distribution of each elementary mode in the given stage; a_{jk} is the time-varying combined flux through all elementary modes; and x_{0jk} represents the current biomass concentration at the given collocation point. In addition to changes in fractional EFM distribution, the step size h_l is also optimized by the nonlinear program and allowed to vary between fermentation modes.

Solution of the problem involves the constrained optimization over the variables found in Table 2 of the productivity objective

$$\max_{\mathbf{X},\mathbf{Y},\mathbf{A},\mathbf{h}} \frac{x_{p,N_K}(1) - x_{p,0}(0)}{\sum_{j=0}^{N_K}\mathbf{h}(j)}. \tag{5}$$

Orthogonal collocation imposes a number of constraints during the optimization process (eqns. 6, 7, 8, 9, 10). The first of these constraints is that state variable profiles must obey system dynamics, accomplished by ensuring that the derivative of the interpolating polynomial defined in eq. 3 is equal to the dynamics defined in eq. 4 at each collocation point. Limits are also placed on the specific uptake and secretion rates at each collocation point in accordance with biological measurements, and the sum of the fractional expression of each elementary mode for the given fermentation stage is constrained to unity.

$$\begin{aligned} &\text{for } j \in [0, N_K];\ k \in [1, N_D]: \\ &\quad h_l a_{jk} x_{0jk}\mathbf{R}\ \mathbf{y}_l - \sum_{n=0}^{N_D} \frac{d\boldsymbol{\ell}_n(\tau_k)}{d\tau}\mathbf{x}_{jn} = 0 \\ &\quad \mathbf{v_{lb}}(\mathbf{x}_{jk}) \leq a_{jk}\mathbf{R}\ \mathbf{y}_l \leq \mathbf{v_{ub}}(\mathbf{x}_{jk}) \\ &\quad \sum_{m}^{N_R} y_{lm} = 1 \end{aligned} \tag{6}$$

Furthermore, the finite elements are constrained to be continuous:

$$\mathbf{x}_j(1) - \mathbf{x}_{j+1}(0) = 0 \quad \text{for } j \in [0, N_K - 1] \tag{7}$$

Bounds are also placed on each of the optimization variables:

$$\begin{aligned} 0 < \mathbf{X} < 1000 \\ 0 < \mathbf{Y} < 1 \\ 0 < \mathbf{A} < \infty \\ 0.1 < \mathbf{h} < 30 \end{aligned} \tag{8}$$

Finally, two additional constraints are imposed in order to avoid numerical instability and trivial solutions. The relative change in step size between fermentation modes is constrained to a factor of 10,

$$\frac{\mathbf{h}_{\max}}{\mathbf{h}_{\min}} \leq 10, \tag{9}$$

and the fermentation must consume at least 80% of the initial glucose:

$$\frac{x^f_{glc}}{x^0_{glc}} \leq 0.2 \tag{10}$$

Implementation

Metabolic models are specified using cobrapy [Ebrahim et al., 2013]. EFMs for each metabolic model are calculated via efmtool [Terzer and Stelling, 2008]. All calculations were performed in Python, using the CasADi library [Andersson, 2013] to implement the orthogonal collocation method. IPOPT [Wächter and Biegler, 2005] was used to solve the resulting NLP problem.

Results and discussion

We demonstrate the usefulness of the method by calculating the maximum theoretical productivities of succinic acid from glucose for two organisms, *E. coli* and *A. succinogenes*. In a developing a DFBA model, we integrate knowledge of the core-carbon metabolic pathways present in the organism together with experimental data on biomass production and substrate uptake rates. An overview of the computational method is provided in Figure 1.

Core-carbon models of *A. succinogenes* and *E. coli*

A. succinogenes

A stoichiometric model of core-carbon metabolism in *A. succinogenes* was created based on genomic evidence and a previous metabolic reconstruction [McKinlay et al., 2010]. The model consists of 72 metabolites and 89 mass- and charge-balanced reactions. Precursor metabolites for biomass synthesis were taken from an *E. coli* core carbon model [Orth et al., 2010]. From experimental measurements on the specific growth and glucose uptake rates of *A. succinogenes*, 0.414 hr^{-1} and 9.5 mmol respectively [McKinlay et al., 2005], we tailored the growth-assisted maintenance and redox cofactors terms in the biomass equation to match known values. No oxygen uptake was allowed to simulate anaerobic growth. A non-growth-assisted maintenance value of 4.7 mmol $\text{g}_{\text{DCW}}^{-1}\text{hr}^{-1}$ was also enforced, which was determined from the value estimated by Lin and coworkers (2008) by finding the amount of ATP that can be produced from 0.308 g of glucose [Lin et al., 2008].

Dynamic constraints on substrate uptake were also imposed. Substrate and product inhibition on growth rate in *A. succinogenes* have previously been quantified with a Han-Levenspiel model [Lin et al., 2008]. Using the calculated biomass yield of 0.044 g_{DCW} / mmol glucose, the experimentally determined parameters were converted to constraints on glucose uptake:

$$v_{glc,\min} = \frac{v_{\max}\, x_{glc}}{x_{glc} + K_s} \prod_n \left(1 - \frac{x_n}{C^\star_n}\right)^{a_n} \tag{11}$$

The parameters used in the eq. 11 are presented in Table 3. Additionally, the lower bound of the flux through non-growth associated ATP maintenance was constrained to the estimated value:

$$v_{atp,\min} = 4.7$$

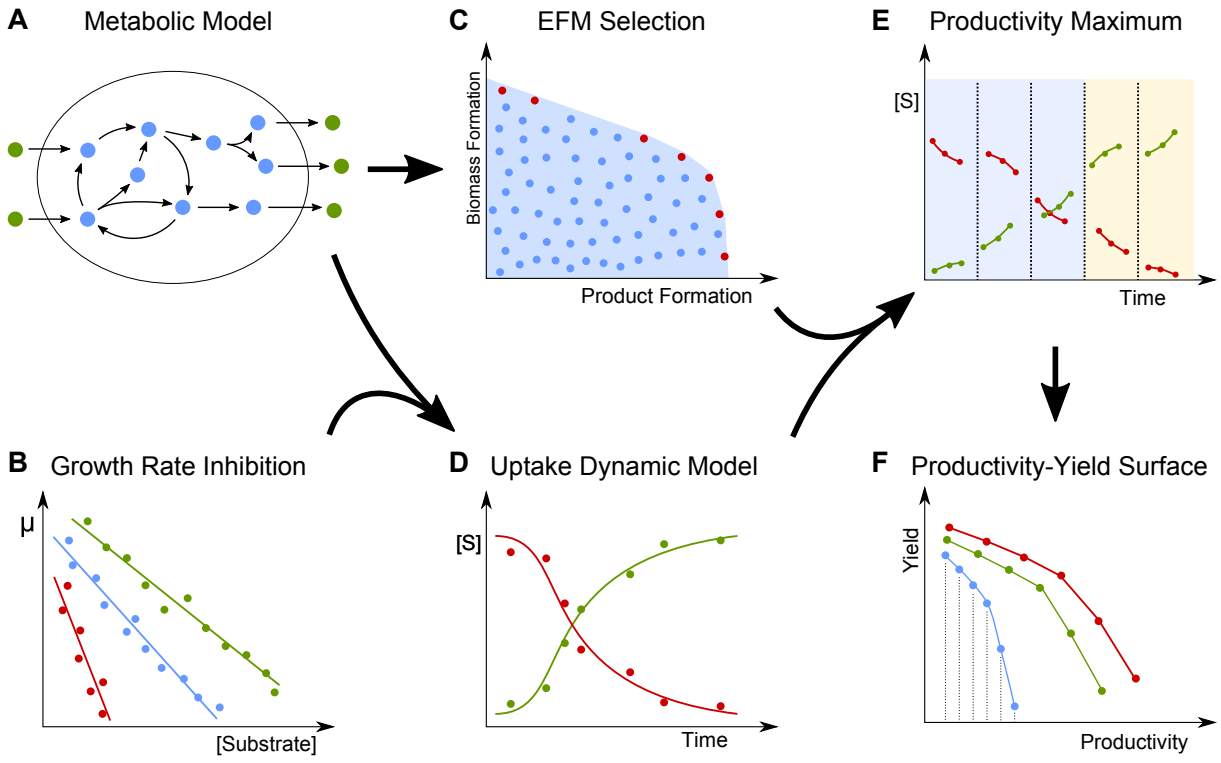

Figure 1: Method Overview. A flow chart for how productivity-yield surfaces are calculated. Stoichiometric metabolic models (*A*) are generated from literature sources or genome annotations and are used to calculate the extreme elementary modes of the system (*C*). Data from growth experiments (*B*) are used together with stoichiometric models to fit dynamic expressions for substrate uptake kinetics and cellular growth (*D*). Bounds on substrate uptake are used with the set of EFMs in dynamic optimization (*E*) in order to calculate optimal flux profiles. This procedure is repeated to maximize product yield for a number of specified productivity constraints (*E*), generating the surface of maximum yield as a function of desired productivity.

Table 3: Parameters for the maximum specific glucose uptake, adapted from values estimated by Lin *et al.* [Lin et al., 2008]

Parameter	Value	Units
$v_{\max}$	-11.47	mmol g_{DCW}^{-1}
K_s	11.27	mM
$C^{\star}_{\text{glucose}}$	860.4	mM
$C^{\star}_{\text{succinate}}$	385.7	mM
$C^{\star}_{\text{formate}}$	235.3	mM
$C^{\star}_{\text{acetate}}$	538.8	mM
a_{glucose}	.603	-
$a_{\text{succinate}}$	1	-
a_{formate}	1	-
a_{acetate}	1	-

E. coli

A core-carbon model for *E. coli* central metabolism was taken from Orth *et al.* [Orth et al., 2010], which consists of 72 metabolites and 94 reactions. Dynamic models for glucose uptake in *E. coli* typically assume Michaelis-Menten kinetics, in which high concentrations of glucose ultimately saturate the import mechanisms at their maximum value [Hanly et al., 2011, Song and Ramkrishna, 2010, Harwood et al., 2015]. However, this assumption leads to the erroneous result that maximum productivity is achieved at an infinite initial glucose concentration. Since no suitable literature model for substrate-level growth inhibition from the considered substrates could be found, glucose uptake kinetics were adapted from those used for *A. succinogenes*. Additional bounds on ATP maintenance and oxygen uptake were adapted from those determined by Feist and coworkers [Feist et al., 2007]:

$$v_{atp,\min} = 8.39$$
$$v_{o2,\min} = -18.2$$

Calculation and selection of elementary models for *A. succinogenes* and *E. coli*

Elementary flux modes were calculated to reduce the dimensionality of the optimization and to alleviate the necessity of enforcing stoichiometric equilibrium constraints during the dynamic optimization. For *A. succinogenes*, 4763 EFMs were calculated for growth on glucose and normalized by the glucose uptake rate. After reducing EFMs to the considered boundary species, duplicate EFMs were removed. The boundary species considered for *A. succinogenes* included biomass, ATP, glucose, succinate, formate, acetate, and pyruvate. Since any feasible flux state can be expressed as a nonnegative combination of elementary flux modes, the flux space in the reduced dimensionality can be spanned without loss of generality by only those EFMs at the vertices of a convex hull. Furthermore, as optimal succinate productivity will be achieved using flux modes on the Pareto front of cell growth, ATP production, and succinate secretion, the reduced set of EFMs were further reduced to a final set of 22 Pareto-optimal modes. As EFMs are normalized by glucose consumption, glucose needs not be explicitly included in the Pareto surface. For *E. coli*, the additional aerobic growth modes led to a total of $100,273$ EFMs. The boundary species for *E. coli* were the same as those used for *A. succinogenes*, with the addition of oxygen and the omission of pyruvate, which was not found to be present in any optimal growth mode. In addition to biomass, ATP, and succinate production, the convex hull of optimal modes in *E. coli* must also consider oxygen consumption. After reduction, 137 modes were kept for *E. coli*.

The selected EFMs for each organism are shown in Figure 2, which plots 2D slices of the 3D (A) and 4D (B) yield surfaces. In *A. succinogenes*, the chosen elementary modes can span the entirety of the yield space for the considered boundary species. In *E. coli*, modes that consume high amounts of oxygen while

yielding low amounts of ATP are omitted by the algorithm, as they are unlikely to be utilized in the optimal productivity solution.

Orthogonal collocation

Optimum productivities are found via a dynamic optimization framework. To further reduce the dimensionality of the optimization, and to allow the effects of discrete fermentation stages to be explicitly simulated, we divide the fermentation time into a number of discrete stages. Within each stage, fluxes are represented by a total flux profile through all elementary modes along with a fractional breakdown of flux through each elementary mode. An example optimum solution for maximum productivity from a 3-stage fermentation in *A. succinogenes* is shown in Figure 3. For clarity, this example uses only 4 finite elements per fermentation stage, while all other calculations use a minimum of 20 total finite elements evenly divided between stages. The figure demonstrates how the step sizes **h** are optimized to achieve the desired dynamic profile. Additionally, since EFMs are scaled by glucose uptake, the activity parameter smoothly tracks the maximum allowable uptake rate. ATP production is enforced at each collocation point by requiring that the flux through the ATP boundary reaction is greater than the non-growth associated maintenance requirement. The selected EFMs in Figure 3B demonstrate that optimal productivity is achieved by prioritizing cell growth early in the fermentation and succinate production in later stages. The elementary mode that represents the maximum theoretical yield for succinate on glucose, 1.71 mol succinate / mol glucose, is used only partially in the last fermentation stage, highlighting that constraints on cell maintenance prohibit the system from achieving the maximum theoretical yield.

Effect of increasing the number of fermentation stages.

In addition to reducing the dimensionality of the problem, splitting the fermentation time into discrete stages with independent EFM expression allows a systematic investigation into the effect of stage count on maximum theoretical productivity. Relative flux ratios within each stage are fixed, and therefore represent consistent enzyme expression. Optimal productivities achieved for a varying number of fermentation stages are shown in Figure 4 for *A. succinogenes* and *E. coli*. The right hand side of Figure 4 plots the dynamic constraints imposed on the solution, including ATP maintenance production rate, maximum glucose uptake rate, and the oxygen uptake rate (for *E. coli*). In all cases, the solutions closely track the maximum allowable glucose uptake rate. In *A. succinogenes*, the transition from one to two stages allows the cell to divide its succinate production strategy into separate growth and product formation stages. The addition of subsequent stages permits slightly higher productivities by the gradual transition from growth to product formation. Additionally, as the flux ratios are fixed within each fermentation stage, the fraction of input carbon diverted to ATP production is also fixed. Thus, as lower extracellular glucose concentrations result in lower glucose uptake rates, the cell must dynamically allocate a higher percentage of energy towards meeting its ATP maintenance requirement. Higher numbers of stages therefore allow the cell to more efficiently meet the maintenance constraint, as demonstrated by lower excess ATP produced with additional stages.

In *E. coli*, maximum succinate production using a single stage is achieved microaerobically. With the addition of a second stage, the optimal fermentation time drops appreciably as succinate production is divided into an aerobic growth phase followed by a microaerobic production phase. The addition of further stages beyond two has little effect on either the succinate productivity or the concentration profiles, serving mainly to keep ATP production closer to the constrained minimum.

Pareto surfaces of yield versus productivity

While separate estimates of maximum theoretical yield and productivity can provide information on the economic feasibility of a bioprocess, in optimized settings one often cannot be increased without decreasing the other. We therefore show how the given method can be easily extended to calculate a full

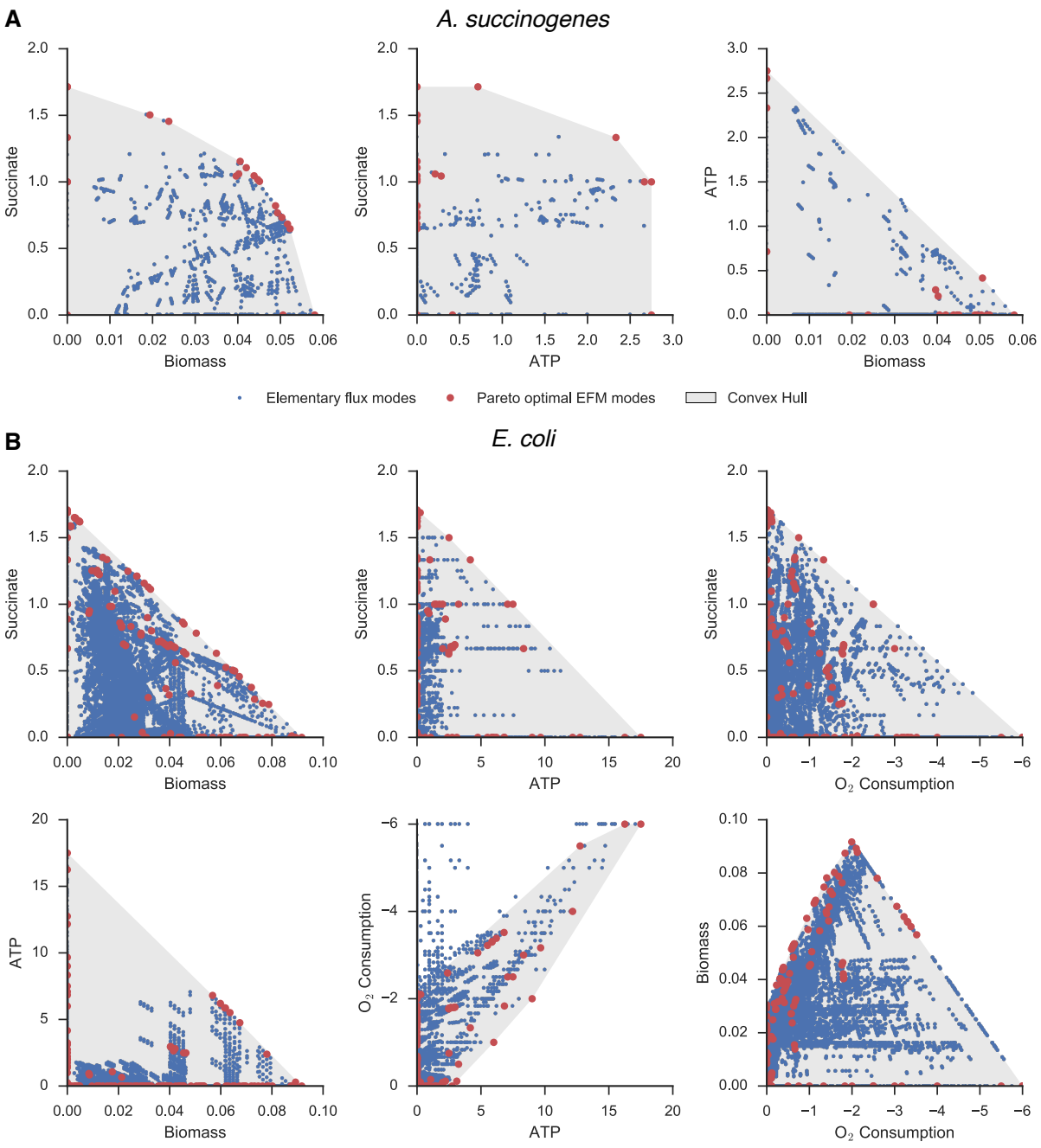

Figure 2: Elementary Flux Mode Surfaces. Projections of the yield surfaces are shown for the 3D yield surface of *A. succinogenes* (*A*) and 4D surface of *E. coli* (*B*). Elementary flux modes are normalized by glucose uptake, and therefore points in yield space represent the amount of product (in mols) which can be produced from 1 mol of glucose. Modes which lie along the Pareto optimal surface are highlighted in red, and the convex hull spanned by these points is shaded gray. For *A. succinogenes*, in which succinate production is coupled to optimal growth, the Pareto frontier of succinate vs. biomass yield is sharply curved. Compared with the corresponding plot in *E. coli*, this shape suggests higher succinate production can be achieved in *A. succinogenes* without a linear penalty in growth and ATP yield. The entire flux cone need not be spanned by the selected EFMs, as demonstrated by the lack of high oxygen consuming - low ATP producing EFMs selected for the *E. coli* network.

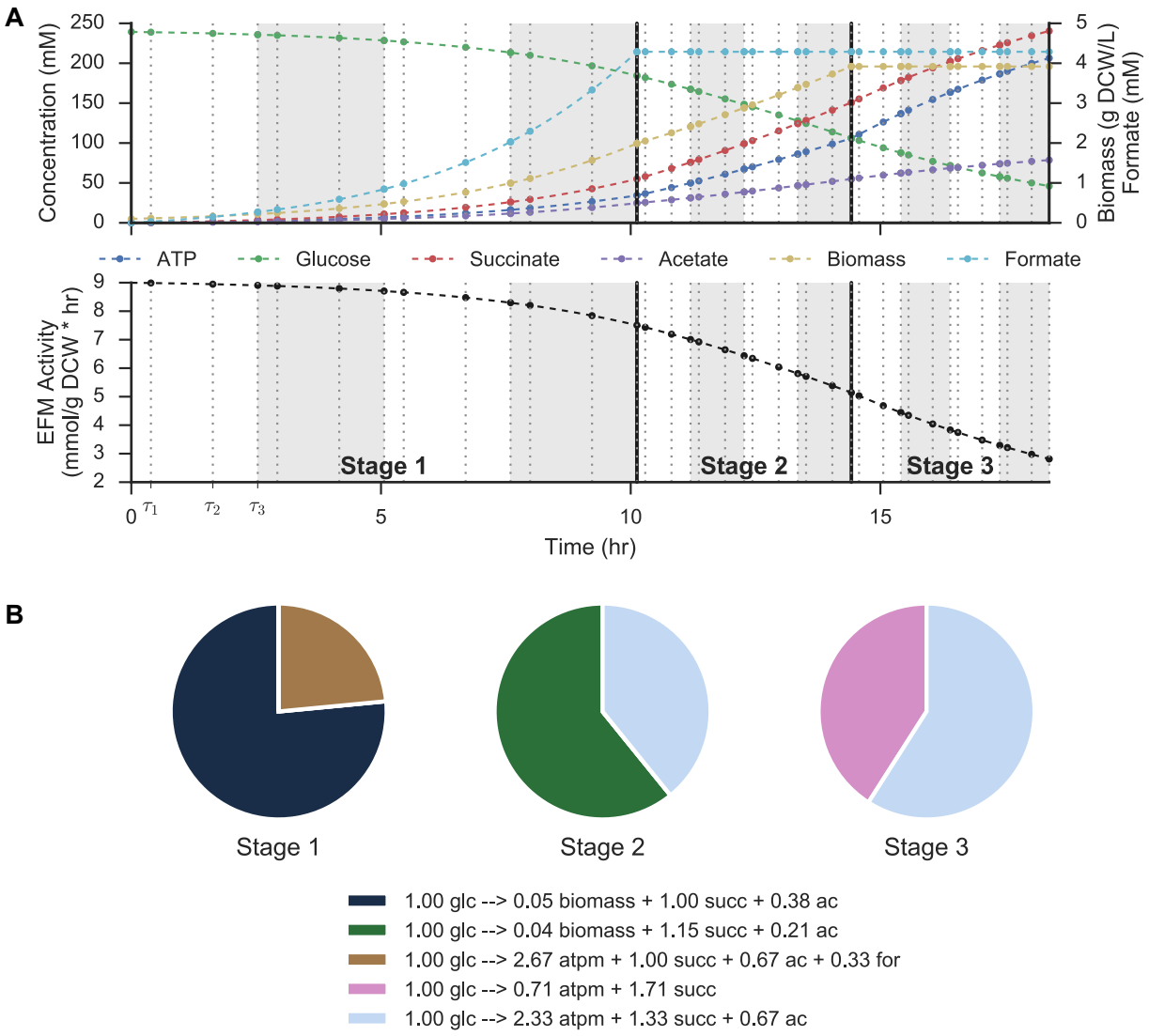

Figure 3: Schematic of the dynamic optimization approach. Example optimum solution for maximum production of succinate in *A. succinogenes*. Time-course trajectories in (*A*) are broken down into three stages, each of which is comprised of a number finite elements (4 in this example, indicated by light/dark shading). Within each finite elements, state variables are represented by a lagrange interpolating polynomial at each of 4 collocation points ($\tau_0 \rightarrow \tau_3$), with continuity constraints between finite elements. The step size of the finite elements, h, within each stage is also optimized. Metabolic fluxes are optimized by simultaneously optimizing the fractional expression of each elementary mode by stage (*B*) with the overall activity of all elementary modes (*A*, lower plot). In this example, high-growth modes are replaced by high succinate yielding modes in later fermentation stages.

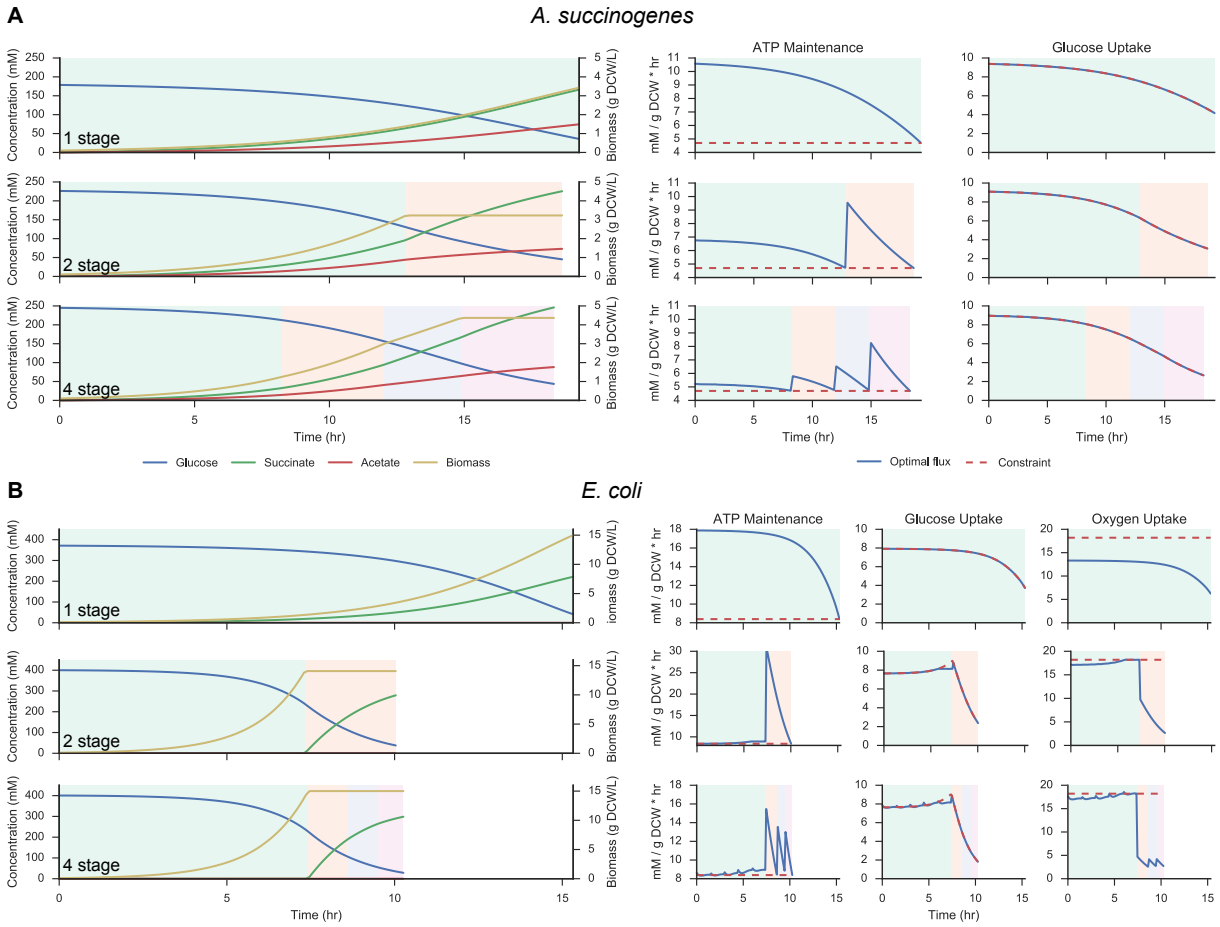

Figure 4: Optimal productivity traces for different numbers of fermentation stages. (*A*) In *A. succinogenes*, additional stages achieve higher titers while only slightly reducing the optimal fermentation time. This result is achieved by prioritizing growth early in the fermentation and succinate production during the later stages. Additionally, the greater flexibility afforded by more stages allows ATP production to be tailored to meet cellular demand, and less ATP is wasted. (*B*) In *E. coli*, additional stages drastically reduce the optimum fermentation time as aerobic growth modes are used to increase biomass ealy in the fermentation. Additional stages beyond two do not drastically change the optimum results, indicating that a simple change from aerobic growth to microaerobic succinate production is close to the global optimum production strategy.

productivity-yield Pareto surface: the envelope in the multi-objective optimization on which productivity cannot be increased without sacrificing yield. The surface is found by first calculating the maximum productivity ($\mathcal{P}_{\max}$, defined by eq. 5) via the method described previously.

The nonlinear program is then resolved with yield as the objective,

$$\max_{\mathbf{X},\mathbf{Y},\mathbf{A},\mathbf{h}} \frac{x_{p,N_K}(1) - x_{p,0}(0)}{x_{g,0}(0) - x_{g,N_K}(1)},$$

in which $\mathbf{x}_g$ represents the glucose concentration, while holding productivity constrained to a fraction of the maximum productivity,

$$\frac{x_p(t_f) - x_p(t_0)}{t_f} - \alpha \mathcal{P}_{\max} = 0 \quad \text{for } \alpha \in [0, 1].$$

Computational efficiency in the repeated optimizations is improved by using IPOPT's warm solve method, which preserves the optimal solution as a starting guess for the next iteration.

Figure 5 plots the resulting yield-productivity surfaces for 50 linearly spaced α values. By varying the number of allowed fermentation stages, these surfaces reveal the performance gains which can be achieved by allowing additional metabolic flexibility. For *A. succinogenes*, higher yields can be obtained due to the lower specific ATP maintenance requirement. Additionally, as succinic acid is the naturally predominant fermentation product in *A. succinogenes*, high yields are obtained even at close to the maximum productivity. In *E. coli*, notable performance gains are achieved by moving to a 2-stage fermentation, as it enables efficient usage of aerobic growth modes. In both cases, moving beyond two distinct flux modes does not substantially increase the yields or productivities that can be achieved.

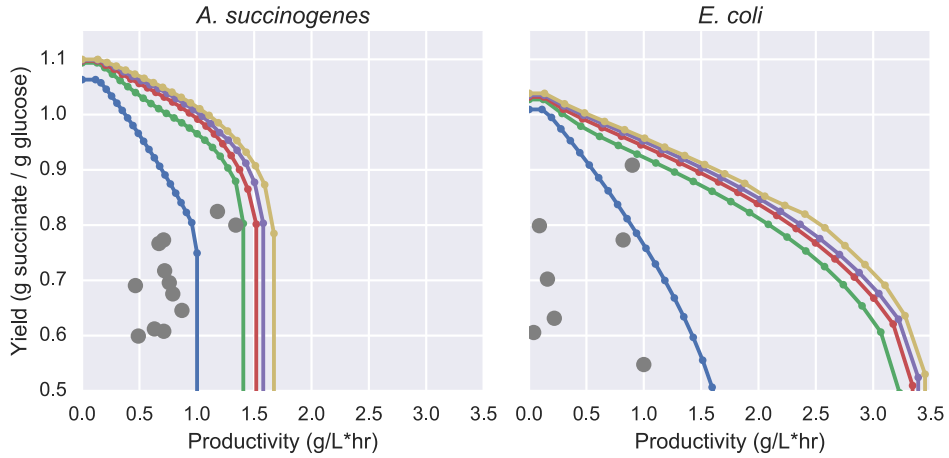

Figure 5: Productivity-yield pareto surfaces for *A. succinogenes* and *E. coli*. Productivity-yield surfaces are calculated by holding productivity constant while maximizing yield for a given number of stages. Experimentally realized productivity and yields are shown in gray, with most points falling in the space predicted by single-stage strategies. References for the experimental points are given in Table 4 and Table 5 for *A. succinogenes* and *E. coli*, respectively. The results indicate that improving existing yields in *A. succinogenes* fermentations would lead to greater gains than improving productivity. Similarly in *E. coli*, the results show that higher productivities could likely be achieved by leveraging aerobic growth modes more effectively.

The calculated optimal surfaces are compared to data on succinate yield and productivity that have been achieved experimentally from both wild-type and engineered organisms, compiled in Tables 4, 5. The data largely fall within the predicted envelope of single-stage processes, confirming the accuracy of the assumptions made in each model. These results illustrate how the proposed method can be useful

for guiding experimental effort: as wild-type *A succinogenes* fermentations naturally fall close to the optimal productivity-yield surface, further genetic manipulation of this organism is unlikely to yield significantly improved performance. Similarly with *E. coli*, improving succinate productivity beyond the values previously recorded will likely require a two-stage process involving aerobic growth and anaerobic succinate production.

Table 4: Literature data for productivity and yield achieved in *A. succinogenes* batch fermentations.

Productivity (g/L*hr)	Yield (g/g)	Reference
1.18	0.82	[Li et al., 2010]
0.71	0.77	[Li et al., 2010]
0.49	0.60	[Li et al., 2010]
0.67	0.77	[Li et al., 2010]
0.76	0.70	[Li et al., 2010]
0.63	0.61	[Li et al., 2010]
0.46	0.69	[Salvachúa et al., 2016]
0.72	0.72	[Salvachúa et al., 2016]
0.71	0.61	[Salvachúa et al., 2016]
0.87	0.65	[Salvachúa et al., 2016]
0.55	0.76	[Guettler et al., 1996]
1.34	0.80	[Guettler et al., 1996]

Table 5: Literature data for productivity and yield achieved in *E. coli* batch fermentations.

Productivity (g/L*hr)	Yield (g/g)	Reference
0.90	0.91	[Jantama et al., 2008]
0.82	0.77	[Jantama et al., 2008]
1.27	0.46	[Andersson et al., 2007]
0.60	0.28	[Millard et al., 1996]
0.22	0.63	[Stols and Donnelly, 1997]
1.00	0.55	[Lin et al., 2005]
0.16	0.70	[Lin et al., 2005]
0.09	0.80	[Sánchez et al., 2005]
0.04	0.61	[Sánchez et al., 2005]

Conclusions

This study represents a computationally efficient method for determining the maximum theoretical productivity for a batch culture system. As the fields of metabolic engineering and synthetic biology continue to develop techniques for the dynamic manipulation of metabolism, our methodology will enable experimental efforts to be focused on where the greatest improvements can be expected. While this study has focused on finding globally optimal solutions, future implementations might search for optimal strategies using only experimentally tractable EFM selections (i.e., ones that are growth-optimal for 1 or 2 gene knockouts). The method can also easily be generalized for conversion of multiple substrates as long as appropriate experimental data exists to fit detailed models to substrate uptake kinetics. It could also be extended to explicitly optimize final titer instead or in addition to yield and productivity. Overall, this work emphasizes the need for better empirical models of substrate and product exchange rates and growth kinetics in designing dynamic metabolic interventions.

Declarations

Ethics approval and consent to participate

Not applicable

Consent for publication

Not applicable

Availability of data and material

The datasets generated during and/or analysed during the current study are available in the github repository, `https://github.com/pstjohn/productivity-maximization`

Competing interests

The authors declare that they have no competing interests

Funding

This work was funded by the US Department of Energy's Bioenergy Technologies Office (DOE-BETO), Contract No. DE-AC36-08GO28308 with the National Renewable Energy Laboratory

Authors' contributions

PSJ, YJB, and MFC designed the method and wrote the manuscript. PSJ performed all numerical experiments. All authors read and approved the final manuscript.

Acknowledgements

We thank Gregg Beckham for his careful review of the manuscript.

References

C Andersson, D Hodge, K A Berglund, and U Rova. Effect of different carbon sources on the production of succinic acid using metabolically engineered Escherichia coli. *Biotechnol Progr*, 23(2):381–388, apr 2007. doi: 10.1021/bp060301y.

J Andersson. A general-purpose software framework for dynamic optimization. *Arenberg Doctoral School*, 2013.

Nikolaos Anesiadis, William R Cluett, and Radhakrishnan Mahadevan. Dynamic metabolic engineering for increasing bioprocess productivity. *Metab Eng*, 10(5):255–266, sep 2008. doi: 10.1016/j.ymben.2008.06.004.

Lorenz T Biegler. An overview of simultaneous strategies for dynamic optimization. *Chem Eng Process*, 46 (11):1043–1053, nov 2007. doi: 10.1016/j.cep.2006.06.021.

Lorenz T Biegler. *Nonlinear Programming*. Society for Industrial and Applied Mathematics, 2010. ISBN 978-0-89871-702-0. doi: 10.1137/1.9780898719383.ch10.

Anthony P Burgard, Priti Pharkya, and Costas D Maranas. Optknock: A bilevel programming framework for identifying gene knockout strategies for microbial strain optimization. *Biotechnol Bioeng*, 84(6):647–657, 2003. doi: 10.1002/bit.10803.

R Davis, L Tao, E C D Tan, M J Biddy, G T Beckham, C Scarlata, J Jacobson, K Cafferty, J Ross, J Lukas, D Knorr, and P Schoen. Process design and economics for the conversion of lignocellulosic biomass to hydrocarbons: Dilute-acid and enzymatic deconstruction of biomass to sugars and biological conversion of sugars to hydrocarbons. Technical Report NREL/TP-5100-60223, oct 2013. doi: 10.2172/1107470.

Ali Ebrahim, Joshua A Lerman, Bernhard Ø Palsson, and Daniel R Hyduke. Cobrapy: Constraints-based reconstruction and analysis for python. *BMC Syst Biol*, 7(1):74, 2013. doi: 10.1186/1752-0509-7-74.

Adam M Feist, Christopher S Henry, Jennifer L Reed, Markus Krummenacker, Andrew R Joyce, Peter D Karp, Linda J Broadbelt, Vassily Hatzimanikatis, and Bernhard Palsson. A genome-scale metabolic reconstruction for Escherichia coli K-12 MG1655 that accounts for 1260 ORFs and thermodynamic information. *Mol Syst Biol*, 3(121):121, 2007. doi: 10.1038/msb4100155.

Adam M Feist, Markus J Herrgård, Ines Thiele, Jennie L Reed, and Bernhard Ø Palsson. Reconstruction of biochemical networks in microorganisms. *Nat Rev Microbiol*, 7(2):129–143, feb 2009. doi: 10.1038/nrmicro1949.

Kapil G Gadkar, Francis J Doyle III, Jeremy S Edwards, and Radhakrishnan Mahadevan. Estimating optimal profiles of genetic alterations using constraint-based models. *Biotechnol Bioeng*, 89(2):243–251, 2004. doi: 10.1002/bit.20349.

M V Guettler, M K Jain, and D Rumler. Method for making succinic acid, bacterial variants for use in the process, and methods for obtaining variants. US Patent Office, 1996.

T J Hanly and M A Henson. Dynamic metabolic modeling of a microaerobic yeast co-culture: predicting and optimizing ethanol production from glucose/xylose mixtures. *Biotechnol Biofuels*, 6(1):44, 2013. doi: 10.1186/1754-6834-6-44.

Timothy J Hanly, Morgan Urello, and Michael A Henson. Dynamic flux balance modeling of S. cerevisiae and E. coli co-cultures for efficient consumption of glucose/xylose mixtures. *Appl Microbiol Biotechnol*, 93(6):2529–2541, oct 2011. doi: 10.1007/s00253-011-3628-1.

Stuart M Harwood, Kai Höffner, and Paul I Barton. Efficient solution of ordinary differential equations with a parametric lexicographic linear program embedded. *Numer Math*, jul 2015. doi: 10.1007/s00211-015-0760-3.

Jared L Hjersted and Michael A Henson. Optimization of fed-batch saccharomyces cerevisiae fermentation using dynamic flux balance models. *Biotechnol Progr*, 22(5):1239–1248, sep 2006. doi: 10.1021/bp060059v.

K Höffner, S M Harwood, and P I Barton. A reliable simulator for dynamic flux balance analysis. *Biotechnol Bioeng*, 110(3):792–802, oct 2012. doi: 10.1002/bit.24748.

William J Holtz and Jay D Keasling. Engineering static and dynamic control of synthetic pathways. *Cell*, 140(1):19–23, jan 2010. doi: 10.1016/j.cell.2009.12.029.

Kaemwich Jantama, M.J. Haupt, Spyros A. Svoronos, Xueli Zhang, J.C. Moore, K.T. Shanmugam, and L.O. Ingram. Combining metabolic engineering and metabolic evolution to develop nonrecombinant strains of Escherichia coli C that produce succinate and malate. *Biotechnol Bioeng*, 99(5):1140–1153, 2008. ISSN 1097-0290. doi: 10.1002/bit.21694.

Dimitrije Jevremovic, Cong T Trinh, Friedrich Srienc, and Daniel Boley. On algebraic properties of extreme pathways in metabolic networks. *J Comput Biol*, 17(2):107–119, 2010. doi: 10.1089/cmb.2009.0020.

J Li, M Jiang, K Q Chen, Q Ye, L A Shang, and P Wei. Effect of redox potential regulation on succinic acid production by Actinobacillus succinogenes. *Bioprocess Biosyst Eng*, 33(8):911–920, 2010. doi: 10.1007/s00449-010-0414-x.

Henry Lin, George N Bennett, and Ka-Yiu San. Metabolic engineering of aerobic succinate production systems in Escherichia coli to improve process productivity and achieve the maximum theoretical succinate yield. *Metab Eng*, 7(2):116–127, mar 2005. doi: 10.1016/j.ymben.2004.10.003.

Sze Ki Carol Lin, Chenyu Du, Apostolis Koutinas, Ruohang Wang, and Colin Webb. Substrate and product inhibition kinetics in succinic acid production by Actinobacillus succinogenes. *Biochem Eng J*, 41(2):128–135, sep 2008. doi: 10.1016/j.bej.2008.03.013.

Radhakrishnan Mahadevan, Jeremy S Edwards, and Francis J Doyle III. Dynamic flux balance analysis of diauxic growth in Escherichia coli. *Biophys J*, 83(3):1331–1340, sep 2002. doi: 10.1016/S0006-3495(02)73903-9.

James B McKinlay, J Gregory Zeikus, and Claire Vieille. Insights into *Actinobacillus succinogenes* fermentative metabolism in a chemically defined growth medium. *Appl Environ Microb*, 71(11):6651–6656, 2005. doi: 10.1128/AEM.71.11.6651-6656.2005.

James B McKinlay, Maris Laivenieks, Bryan D Schindler, Anastasia a McKinlay, Shivakumara Siddaramappa, Jean F Challacombe, Stephen R Lowry, Alicia Clum, Alla L Lapidus, Kirk B Burkhart, Victoria Harkins, and Claire Vieille. A genomic perspective on the potential of Actinobacillus succinogenes for industrial succinate production. *BMC Genomics*, 11(1):680, 2010. doi: 10.1186/1471-2164-11-680.

C S Millard, Y P Chao, J C Liao, and M I Donnelly. Enhanced production of succinic acid by overexpression of phosphoenolpyruvate carboxylase in Escherichia coli. *Appl Environ Microb*, 62(5):1808–1810, may 1996.

Jeffrey D Orth, R M T Fleming, and Bernhard Ø Palsson. Reconstruction and use of microbial metabolic networks: the core Escherichia coli metabolic model as an educational guide. *EcoSal Plus*, 4(1), sep 2010. doi: 10.1128/ecosalplus.10.2.1.

Sridhar Ranganathan, Patrick F Suthers, and Costas D Maranas. Optforce: An optimization procedure for identifying all genetic manipulations leading to targeted overproductions. *Plos Comput Biol*, 6(4):e1000744–11, apr 2010. doi: 10.1371/journal.pcbi.1000744.

David E Ruckerbauer, Christian Jungreuthmayer, and J u rgen Zanghellini. Design of optimally constructed metabolic networks of minimal functionality. *PLoS ONE*, 9(3), 2014. doi: 10.1371/journal.pone.0092583.

Davinia Salvachúa, Ali Mohagheghi, Holly Smith, Michael F A Bradfield, Willie Nicol, Brenna A Black, Mary J Biddy, Nancy Dowe, and Gregg T Beckham. Succinic acid production on xylose-enriched biorefinery streams by Actinobacillus succinogenes in batch fermentation. *Biotechnol Biofuels*, 9(1):121, feb 2016. doi: 10.1186/s13068-016-0425-1.

Ailen M Sánchez, George N Bennett, and Ka-Yiu San. Novel pathway engineering design of the anaerobic central metabolic pathway in Escherichia coli to increase succinate yield and productivity. *Metab Eng*, 7(3):229–239, may 2005. doi: 10.1016/j.ymben.2005.03.001.

S Schuster, T Dandekar, and D A Fell. Detection of elementary flux modes in biochemical networks: a promising tool for pathway analysis and metabolic engineering. *Trends Biotechnol*, 17(2):53–60, 1999. doi: 10.1016/s0167-7799(98)01290-6.

Yuki Soma, Keigo Tsuruno, Masaru Wada, Atsushi Yokota, and Taizo Hanai. Metabolic flux redirection from a central metabolic pathway toward a synthetic pathway using a metabolic toggle switch. *Metab. Eng.*, 23:175–184, may 2014. doi: 10.1016/j.ymben.2014.02.008.

Hyohak Song and Sang Yup Lee. Production of succinic acid by bacterial fermentation. *Enzyme Microb Tech*, 39(3):352–361, jul 2006. doi: 10.1016/j.enzmictec.2005.11.043.

Hyun-Seob Song and Doraiswami Ramkrishna. Reduction of a set of elementary modes using yield analysis. *Biotechnol Bioeng*, 102(2):554–568, feb 2009. doi: 10.1002/bit.22062.

Hyun-Seob Song and Doraiswami Ramkrishna. Cybernetic models based on lumped elementary modes accurately predict strain-specific metabolic function. *Biotechnol Bioeng*, 108(1):127–140, oct 2010. doi: 10.1002/bit.22922.

L Stols and M I Donnelly. Production of succinic acid through overexpression of NAD(+)-dependent malic enzyme in an Escherichia coli mutant. *Appl Environ Microb*, 63(7):2695–2701, jul 1997.

Marco Terzer and Jörg Stelling. Large-scale computation of elementary flux modes with bit pattern trees. *Method Biochem Anal*, 24(19):2229–2235, 2008. doi: 10.1093/bioinformatics/btn401.

Norma A Valdez-Cruz, Luis Caspeta, Néstor O Pérez, Octavio T Ramírez, and Mauricio A Trujillo-Roldán. Production of recombinant proteins in E. coli by the heat inducible expression system based on the phage lambda pl and/or pr promoters. *Microb Cell Fact*, 9(1):1, mar 2010. doi: 10.1186/1475-2859-9-18.

Naveen Venayak, Nikolaos Anesiadis, William R Cluett, and Radhakrishnan Mahadevan. Engineering metabolism through dynamic control. *Curr Opin Biotechnol*, 34:142–152, aug 2015. doi: 10.1016/j.copbio.2014.12.022.

Andreas Wächter and Lorenz T Biegler. On the implementation of an interior-point filter line-search algorithm for large-scale nonlinear programming. *Math Program*, 106(1):25–57, apr 2005. doi: 10.1007/s10107-004-0559-y.

Kai Zhuang, Laurence Yang, William R Cluett, and Radhakrishnan Mahadevan. Dynamic strain scanning optimization: an efficient strain design strategy for balanced yield, titer, and productivity. dyssco strategy for strain design. *BMC Biotechnol*, 13(1):8, 2013. doi: 10.1186/1472-6750-13-8.